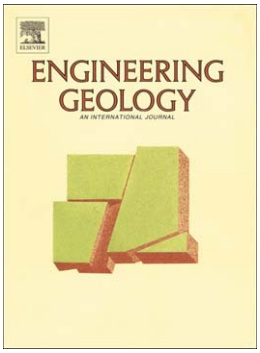

Three dimensional characterization of complex mantled karst structures. Decision making and engineering solutions applied to a road overlying evaporite rocks in the Ebro Basin (Spain)

Ó. Pueyo Anchuela, P. López Julián, A.M. Casas Sainz, C.L. Liesa, A. Pocoví Juan, J. Ramajo Cordero, J.A. Pérez Benedicto

PII: S0013-7952(15)00138-6
DOI: doi: 10.1016/j.enggeo.2015.04.022
Reference: ENGEO 4030

To appear in: *Engineering Geology*

Received date: 27 January 2015
Revised date: 10 April 2015
Accepted date: 26 April 2015

Please cite this article as: Pueyo Anchuela, Ó., López Julián, P., Casas Sainz, A.M., Liesa, C.L., Pocoví Juan, A., Ramajo Cordero, J., Pérez Benedicto, J.A., Three dimensional characterization of complex mantled karst structures. Decision making and engineering solutions applied to a road overlying evaporite rocks in the Ebro Basin (Spain), *Engineering Geology* (2015), doi: 10.1016/j.enggeo.2015.04.022

Title: *"Three dimensional characterization of complex mantled karst structures. Decision making and engineering solutions applied to a road overlying evaporite rocks in the Ebro Basin (Spain)"*

Authors: Pueyo Anchuela, Ó., [1, *]; López Julián, P. [2], Casas Sainz, A.M. [1], Liesa, C.L. [1], Pocoví Juan, A. [1], Ramajo Cordero, J. [1], Pérez Benedicto, J.A [2]

(1) Departamento de Ciencias de la Tierra. Universidad de Zaragoza.

(2) Escuela Universitaria Politécnica de La Almunia. Universidad de Zaragoza.

(*) Corresponding author: Óscar Pueyo Anchuela. Área de Geodinámica Interna. Departamento de Ciencias de la Tierra. Universidad de Zaragoza. C/ Pedro Cerbuna, nº 12. CP. 50.009. Zaragoza. Spain. opueyo@unizar.es. Phone 0034976762127. Fax 0034976761106.

Abstract

At mantle/cover evaporite karst settings, evidences of surficial subsidence are usually strongly dependent on geomechanical properties and spatial inhomogeneities within the cover series. In infrastructures assets, affected by karst processes, the evaluation of mitigation or engineering solutions requires a 3D reconstruction of the underground, karst-affected materials. Analysis and surveillance are also required to avoid deterioration of natural conditions and the migration or the increase in rate of karst features. In the central Ebro Basin, fluvial deposits cover soluble salts (mainly gypsum) located below the regional water table. Variations of geomechanical parameters of the cover, mainly related to carbonate crusts, and the contemporaneous sedimentation of fluvial deposits during karst activity can complicate the characterization of affected volumes. In this work, an integrated analysis including the available information, 3D characterization by means of GPR and three boreholes in a peri-

urban road was carried out to finally define the geometry and evolution of karst phenomena. An evaluation of metastable situations is also considered in order to define the zoning for hazard mitigation. This evaluation shows that the volumetric affection to the cover series is in the range of tens of thousands of cubic meters. A proposed list of factors related to social aspects, infrastructure relevance and budget is analyzed.

Keywords: Mantled karst, Ebro Basin, GPR, 3D characterization, foundation analysis, decision-making, evaporite karst.

1. Introduction

Construction on active karst settings and mitigation of its effects on infrastructures and buildings is a complex engineering task. This complexity is related to the karst structure that involves soluble materials in the subsoil and its propagation to the overlying insoluble materials, both consolidated and unconsolidated. The geomechanical characteristics of the series (cohesive, non cohesive or with interbedded caprocks) can produce complex scenarios. The volume affected by karst needs to be defined prior the application of any engineering solution.

Karst, in a general manner, is related to the presence of a soluble material in the subsoil that can be submitted to solution, generating a volume reduction in the underground. The propagation of this reduction to the surface, progressively or instantaneously, through consolidated or unconsolidated materials and depending on its size, produces surficial subsidence processes. These subsidence processes can produce dolines or sinkholes generating topographic depressions and collapses. Carbonate rocks can be affected both by karst and weathering processes and they present a worldwide extension. While climatic conditions can reduce the karst development in northern America, Russia or Africa, usual problems are known at populated areas in the USA, China or Yugoslavia (Waltham et al., 2005). However, evaporites present solubilities several orders of magnitude higher than carbonate rocks. These rocks represent one of the most problematic terrains to perform construction activities (e.g., Johnson and Neal, 2003; Waltham et al., 2005). This kind of terrains occupies 20% of the world´s land surface (Kozary et al., 1968) and they are below other non soluble rocks in the 90% of the cases. Their high solubility produces a usual interaction with infrastructures within their period of service. In the case of Spain, 7% of the country is covered by evaporite materials (Macau and Riba, 1962: Gutiérrez et al., 2008).

In mantled karst, evaporites are below other soils and rocks, usually non soluble, and consequently karst surficial evidences depend on the rheology and thickness of the cover materials. In this sense, different interrelated processes can produce bedrock -inter and intra-stratal dissolution or it can progress through the contact between cover and soluble materials. The results of this dissolution process is the generation of cavities, rock collapses, soil down-washing or soil collapses (Waltham et al., 2005; Gutiérrez et al., 2008).

Karst areas can be analyzed through different approaches progressing from the accurate sizing and mechanism identification and the further definition of investigation and solution proposals (e.g. Kannan, 1999; Lamont-Black et al., 2002). After the problem definition, the decision making can progress through: i) relocation of the proposed construction out of areas having karst activity, and where this is not possible, solutions can be focused on ii) the mitigation by correction of the subsurface materials (grouting, cap grouting, dynamic compaction), iii) the modification of the previously proposed foundation design (rigid mats, deep foundations including driven piles and drilled shafts), iv) the karst factor evaluation in order to avoid new, or the increase of previously identified, subsidence foci (Sowers, 1986; 1996 Greenfield and Shen, 1992: Kannan, 1999; Paukštys et al., 1999; Zhou and Beck, 2008), and in many cases v) after construction control to avoid future karst affection (e.g., Marker, 2010).

Geological information can be used to define the most suitable areas for infrastructure constructions. This approach can be benefited from geomorphological and historical studies, the evaluation of factors influencing karst development and the creation of susceptibility maps (e.g., Simón and Soriano, 2002; Zhou et al., 2003; Gao et al., 2005; Lamelas et al., 2008; Galve et al., 2009; Thierry et al., 2009; Marker, 2010 among others). These approaches are important during urban design and planning; however, in some cases, the infrastructure needs to be located at high susceptibility karst areas or in other cases, the surficial evidences appear after

the infrastructure construction. In such cases, the most prone solution for avoiding the hazardous area is not the easiest solution to be adopted.

In these cases a complete 3D characterization of the underground materials involving the location of the karst origin, the affected volumes of the cover materials and their geomechanical characteristics are needed to design any potential solution or mitigation treatment. In this work, a multi proxy analysis of a sinkhole affecting a road in Gallur town (Ebro basin, Spain) is presented. The presence of collapse sinkholes in the study area is known. The geological and geomorphological analysis permits to know the context of karst origin and to preview the characteristics of potential sinkholes. This analysis is integrated with the topographic leveling, drone flights to obtain a high resolution aerial photography, field inspection, mapping of cracks in the roadway and their distribution, geophysical survey by ground penetrating radar (GPR) and three boreholes employed to constrain the geological model and geotechnical series in the area. These data are used to evaluate the karst-affected volume of underground materials, to evaluate potential mitigation solutions, the decision making approach evaluating cost-benefit solutions and the associated post construction surveillance. This analysis can be of interest not only for the application of such solutions in similar geological contexts; moreover it represents an approach for the analysis at karst complex structures.

2. Geological context

The study area is located in the central sector of the Cenozoic Ebro Basin (NE Spain), which constitutes the endorheic foreland basin of the Pyrenees, the Iberian Chain and the Catalonian Coastal ranges (Fig. 1). During the endorheic stage, it was filled with alluvial (molasse) facies in the marginal areas of the basin grading into lacustrine evaporitic and carbonate sediments towards the central part of the basin (e.g., Quirantes, 1978; Luzón, 2005; Pardo et al., 2004). At the central part of the basin, mainly gypsum but also other more soluble salts exists (e.g., Salvany et al., 2007; Salvany, 2009). The Ebro Basin remained closed at least until middle-late Miocene times, when the endorheic fluvial system opened through the present Ebro River to the Mediterranean (Pérez Rivarés et al., 2002; García Castellanos et al., 2003). A new drainage network started to develop and dissected the endorheic basin fill, generating stepped sequences of mantled pediments and terraces, especially in relation with the Ebro River (Van Zuidam, 1976; Soriano, 1990). These deposits mainly consist of fluvial channel gravels with interbedded sands and clays.

At the central part of the Ebro Depression and overlying Cenozoic evaporites, a complex system of asymmetrical stepped terraces developed. They have a wider extension to the south of the thalweg than to the north (Fig. 1). Fluvial sedimentation took place in some cases synchronously with karst processes affecting the evaporite substratum, as have been suggested by the presence of anomalous geometries and facies within the alluvial series (Luzón et al., 2008: Gil et al., 2013) or anomalous alluvial thickness and the development of aggradational terraces (Benito et al., 1998: Moreno Merino et al., 2008; Pueyo Anchuela et al., 2013). Terrace levels present different geomechanical characteristics depending their age and the presence of pedogenetic and/or phreatic carbonate cementations.

Consequently, sinkholes and dolines are usually found along the central Ebro Basin and especially in the lower terraces where groundwater level is usually over the contact between

the Miocene evaporite substratum and the Quaternary deposits. Karst affects to this system producing mantle karst structures related to the cavity propagation from the substratum to the non soluble cover series involving the whole Quaternary sequence. Surficial processes can be identified as continuous subsidence to sudden collapses structures. Subsidence rates on the order of 0.1-0.2 cm/yr have been quantified at several sinkholes affecting natural domains (Simón et al., 2008; Luzón et al., 2008; Gutiérrez et al., 2011). However, in urbanized domains rates exceed the natural ones with values between 6 and 15 cm/yr (Soriano and Simón, 2002; Pueyo Anchuela et al., 2014a). This rate variation have been related, by Soriano and Simón (2002), to the urbanization changes, the load imprint of construction and traffic, the result of subsidence and sinkhole filling settlement, but also with some of the mitigation measurements that are employed in this setting (e.g. concrete injection). The most usual aspect is the progressive subsidence, however sudden collapses are not rare and in some cases without precursory subsidence (e.g. Gutiérrez et al., 2008; Mochales et al., 2008).

3. Methodology

In order to evaluate the 3D distribution of a karst phenomenon, a sector where surficial evidences affecting to a road in the proximities of the Gallur town was studied (Fig. 1). The studied road was traffic restricted due to the beginning of subsidence and collapse phenomena in 2012. This study has permitted the complete characterization of the underground soil structure and the evaluation of different mitigation proposals.

This study integrates results from historical and geomorphological data, a new drone aerial photograph campaign, a surficial analysis of karst indicators, a GPR systematic survey and data from three drilled boreholes. The study of aerial photographs has been evaluated from 1927 until 2013. A new drone flight devoted to characterize, at high resolution, the studied zone was carried out during 2014. The analysis consisted in the identification of potential indicators of karst processes and anthropogenic modifications. Analyzed aerial

photographs have considered both stereoscopic pairs and orthophotographs. The new flight conducted during 2013 was complemented by the field analysis of the studied zone considering both a topographic leveling and surficial mapping (cracks, topographical slope changes, etc). In the cases of cracks, a kinematic analysis was carried out incorporating slope changes, opening sense and relative movement of fractures. This analysis also included cracks affecting buildings surrounding the studied zone.

The subsurface structure was analyzed by means of ground penetrating radar (GPR) survey that was carried out both at the road and along surrounding accessible areas. GPR has been employed in previous studies for the evaluation of the internal structure of sediments both at undisturbed and karst domains (see Neal, 2004; Pueyo Anchuela et al., 2014b and references therein).

A Ramac CUI-2 device with shielded antennas and central frequencies of 100 and 250 MHz was used for the survey. The profile location was established by GPS at the beginning and the end of the profiles that were carried out along straight lines. The distance along the profiles was established by means of a calibrated wheel plugged to the device. Processing of obtained data consisted in frequency filters, linear and exponential gain, subtract mean trace and migration. The first arrival in the profiles was established during the processing for the subsequent analysis. The propagation velocity was firstly established by the evaluation of the expected materials to be found in the subsoil and later corrected by data obtained from fitting of hyperbolic anomalies (a mean propagation velocity of 110 m/μs was considered). From the GPR data, structural characterization was performed by incorporating slope changes of reflectors in the profiles, sudden lateral interruption of the banded continuity of GPR-profiles and hyperbolic anomalies. This analysis was focused in the identification of accommodation geometries, subsidence phenomena related to reflectors tilting or sudden reflector interruptions as indicators of collapse geometries.

In a second step, two main domains were defined in the GPR profiles: sectors with reflector tilting or modification of the expected original sedimentary structure and sectors where no evident changes of the reflector slope were identified. In some cases, this second domain can present hyperbolic anomalies or sudden lateral interruption of reflectors but without significant changes in the reflector disposition. The position of the contact between both domains was used to construct a spreadsheet where coordinates of each trigger and the TWT coordinate (two way travel time) of the contact were included. After the calculation of the propagation velocity and aided by the topographical leveling, a model of correlation of the TWT (depth) position of this contact was done. The lateral correlation between profiles was established considering the distance between them in order to obtain a 3D model where pixel size is on the order of data distribution. 3D GPR-based model was compared with three new boreholes drilled in different domains, with continuous core logging and standard penetration tests (SPT).

4. Results

The studied zone (Fig. 1) shows a triangular shape defined by the analyzed road and the Imperial Channel of Aragón (an irrigation and navigation channel built during the XVIIIth century) that represents the western limit of the studied zone (Fig. 2a-c). Evidences from different subsidence events have been identified along the last decades from the collapse of a sector from the irrigation channel in 1996 and the road closing in the last years. At surface, the zone is covered by anthropogenic materials and natural soils consisting of clays and gravels. Gravels correspond to the T3 terrace level of the Ebro River (Castiella et al., 1977). In the underground the Miocene Zaragoza Fm (Quirantes, 1978) is expected to be found as it crops out along the northern bank of the Ebro River and to the south and west of the studied area (Fig. 1).

4.1 Field inspection, historical and geomorphological analysis

Aerial photographs, even with stereographic pairs, do not permit to clearly identify topographic changes. Some buildings not observable in the most recent photographs can be identified between the road and the channel (Fig. 2a). The most significant changes occurred between 1984 and 1998 (Fig. 2a,b), when the small buildings disappeared and the sector between the road and the channel was flattened. In this period (possibly in 1996), karst affection to the channel and ruin of a building have been reported by inhabitants. It is interesting to note, that, in 1998 photograph, two topographic depressions, one of them with a differential vegetation growth, can be identified between the road and the channel (Fig. 2b). These topographic changes are not observed in the photographs from 2012 (Fig. 2c) although they could be identified during the field survey. On the road, small topographic depressions are also identified and the most relevant aspect is the presence of semi-circular to semi-elliptical cracks (Fig. 3 a-c). Cracks can be also identified on the road (Fig.3b). The analysis of the neighboring buildings located at the southeastern border of the studied zone also shows

wall cracks pointing to the road having the same dip sense than identified in the road surface (Fig. 3c). The drone flight developed during this work (Fig. 3 d,e,f), permits to define two semi-elliptical topographical depressions that are cut by the road. The surficial analysis shows that the topographic depressions can contain small collapses, (Fig. 3a) and present concentric systems of semicircular cracks affecting the road (Fig. 3d).

In some cases, the topographical changes affecting the road can reach 0.80 m (Fig. 3a). This topographic depression, developed since the last road repair in 2004, has allowed calculating an average subsidence rate between 6 and 9 cm/yr. This subsidence process produced the traffic exclusion from the road in 2012.

Crack analysis and slope changes show different characteristics between the road and the neighboring granular surficial materials. Topographic depressions surrounded by open concentric cracks are observed out of the road, whereas on its surface, some cracks follow concentric patterns. In other cases, cracks progress following construction anisotropies (e.g. interface between concrete and asphalt).

4.2. Ground Penetrating Radar survey

The survey consisted mainly in 20 longitudinal profiles near parallel to road-channel direction in order to avoid topographical changes and to obtain homogeneous results over the same materials (profiles 1 to 20; separated between 3 to 5 meters). Five traverse profiles (profiles 21 to 25) were also carried out in order to refine the obtained data at the sectors that have more evidences of surficial karst (see Fig. 4a for profile location). GPR survey was carried out with 100 and 250 MHz antennas; however, the penetration of 250 MHz in the natural sectors was limited. The comparison of GPR profiles done with both antennas is only of interest in the case of the road, where both resolution and penetration are high (Fig. 4b).

In the different profiles three main features were drawn (Fig. 5c and d): structural changes, sudden lateral interruptions and hyperbolic anomalies. Profiles located over the road (profiles 1 to 4; Fig. 5c) show a high structural complexity. Sudden lateral changes are identified along the whole profile (lateral and vertical distribution) although they do not usually affect to the whole vertical analyzed interval. Between these net changes, especially at the upper part of the profiles and at their southern limit, structural changes affecting to the geometry of upper materials are identified. The highest slopes and structural changes are located at the southern and western part of the road (profiles 3 and 4). Apart from these changes a net reflector is identified at deep conditions along all the profiles (see Fig. 5c). This reflector is clear and independent of the more surficial structural changes and it usually disappears in the southern part of the profiles.

The complexity of GPR profiles at the road contrasts with the profiles performed at the natural domain (between the road and the channel; Fig. 5d). These profiles show a homogeneous structure out of the topographic depressions. This aspect supports that complex structure is related to sectors with karst evidences.

4.3 Borehole data

Three boreholes were drilled in order to ground truth the geophysical anomalies and surficial karst evidences (Fig. 4a): S0 in the central zone of a collapse area where the highest subsidence is identified, S1 in the subsidence ring surrounding one of the collapses and S2 at a sector without evidences of karst affection (both from the geophysical and surficial analysis). The sequence at S0 is composed from top to base by: i) the road at surface, and anthropogenic materials that can reach 7 m and are absent in the rest of the boreholes; ii) alluvial-fluvial unit composed by gravels and sands that can be locally cemented by carbonate (carbonate crusts) and clays at its base; and iii) weathered substratum composed by clays, marls and detrital deposits.

Results from SPT tests (Fig. 5) show, in general, middle to high values at the fluvial deposits (that cannot be penetrated at the carbonatic crusts). In S0 anthropogenic materials show middle to high strength in the upper part of the series, and very low strength in its lower part. Borehole correlation shows, in the granular materials, a change in the resistance of 6 to 14 blows for the intermediate analyzed range (central 30 cm, N30) in S0 against 30 to 75 at the rest of the essays. Below these units, the strength of the clayey materials and upper part of the substratum show middle to low values (fig. 5). Water level shows differences of more than 5 m in depth within horizontal distances of 20 m. The water table is identified over the substratum and the alluvial series in S0 and S2 and within the substratum at S1. It is interesting to note that water wells for factories located directly to the east of the studied zone found a saline water table at depths below 33 m.

5. Interpretation and 3D evaluation

GPR profiles and boreholes results were compared in order to analyze the GPR data and to evaluate the propagation velocity used for the TWT-depth calculation. The structural changes located in the southern domain show a clear correspondence with the increase of anthropogenic materials observed in S0 borehole. Carbonate crusts can be correlated with some of the reflectors at the profiles, but no clear correspondences between GPR units and levels identified at boreholes can be established. Another interesting aspect is the coincidence between the water table in the boreholes and the deep reflector identified in the GPR profiles (note that in the correlation shown in fig. 6a boreholes have been projected for their representation and the position of the water table presents a sharp lateral change).

Although there is not a clear correlation between identified units at boreholes and GPR-profiles, there are structural changes affecting to the terrace and anthropogenic units. In order to evaluate the 3D distribution of these changes, two different structural units have been differentiated in the GPR profiles (Fig. 6b). In the upper unit reflectors are dipping, lose

lateral continuity or show onlap-wedge and symmetrical accommodation geometries. This unit can be present throughout the surveyed zone. The lower unit is characterized by structural changes that present subhorizontal distribution. The contact between both units separates domains with tilted reflectors from more homogeneous, undisturbed, sectors (Fig. 6b). The geometry and distribution of this contact show progressive depth changes with topographic depressions defining plane-concave geometries or subvertical limits. This contact was used for the construction of the 3D model (Fig. 7a).

The 3D model was obtained considering an interpolation in the range of the distance between profiles. This gridding permitted to establish a geometrical model that defines two sectors where tilted reflectors define plane-concave geometries in 2D profiles or 3D bowl shaped geometries. They present zones limited by sudden changes of reflector slopes or by lateral net interruptions of the underground structure, interpreted as collapse structures. It is in these collapse structures where the highest depth to disturbed materials is reached. These structures are surrounded by sectors where tilted reflectors are restricted to changes in the shallow soil with centripetal patterns but without a direct vertical underground connection (subsidence rings in Fig. 7a). If model is enriched with borehole information, collapse geometries can be prolonged over 12 m (Fig. 7b), and subsidence rings reach shallower depths and wider surficial extensions. Within these subsidence envelopes, different rings can be defined depending upon the reflector slopes (inner and external rings). The model shows a clear parallelism with topographical changes and cracks in the natural domain, but correlation is worse in the urban domain (Fig. 7c). In some cases, the cracks on the road followed construction anisotropies presenting irregular trends, while in cases of concentric cracks previously identified (Fig. 3b and d), the model follows this surficial trend.

The integrated analysis with the SPT data permits to identify the presence of a disturbed gradient, with low values at the lower level of anthropogenic and natural materials

in S0 borehole. This evidence happens at a surficial collapse structure where the more pronounced topographic depression of deformed or tilted reflectors is identified. In the rest of the boreholes, although there are structural changes at the GPR profiles, the resistance of the materials, is in general, medium to high. Structural changes were identified in the upper part of the series, but in some cases there are not direct vertical connections of these changes with collapse geometries below them. This can be interpreted as the result of an irregular behavior of the cover series, without propagation of collapses in the underground directly to the surface, except for the southern zone (S0). In the case of S1, the log does not show clear evidences of a sinkhole, but structural changes, surficial cracks and topographical changes indicate the presence of a subsidence process in this zone.

6. Discussion

Subsidence phenomena have been classified based on surficial evidences, underground interpretation and/or involved processes (e.g. Williams, 2003; Beck, 2004; Waltham et al., 2005; Gutiérrez et al., 2008; Pueyo Anchuela et al., 2009). In many cases these classifications require the 3D evaluation and the interpretation of the underground origin from surficial evidences. In terms of the analysis of the subsidence phenomena and its geotechnical or engineering evaluation, besides the previously mentioned aspects, depth to the original cavity, rheology of the different involved materials, presence of caprocks and the alluvial thickness must be considered.

6.1. Evaluation of the subsidence phenomena

The identification of the origin subsidence phenomena constrained only by the surficial evidences can be, in some cases, non-straightforward. The same surficial evidences can be interpreted as a dropout or suffusion doline in relation to a cover drop into a cave, to a fissure or a group of them, following terminology of Waltham et al. (1995). The presence of geomechanical changes within the cover series (e.g. cemented levels) can difficult surficial

interpretation because caprocks can modify the expected vertical propagation of the cavity. The surficial aspect of dropout sinkholes, breccia pipes or caprock collapses are more dependent on the cover properties than on their in-depth actual origin.

These classifications imply considerations about the affected volume and the expected future progression (Fig. 8). The propagation of cavities through cover materials unable to migrate can produce the generation of a dome-shaped vault and shear faulting and tension fractures (Ferrero et al., 2010; Parise and Lollino, 2011; Shalev and Lyakhovsky, 2012), but at levels with high migration potential (low viscosity) the progression produces the generation of a smoothly sloping depression that evolves increasing its radius (Shalev and Lyakhovsky, 2012). In this situation, a metastable stage (Fig. 8) can be defined until sinkhole walls reach the equilibrium according to the internal angle of friction (inverse Gaussian profile at pure non cohesive materials; e.g. Peck, 1969). These analyses also permit to constrain sectors where precursory subsidence should be identified depending upon the viscoelastic properties (e.g Shalev and Lyakhovsky, 2012). The evolution of subsidence foci and the involved processes consider: downwashing of unconsolidated sediments (Cooper, 1986; Paukštys et al., 1997); gradual collapse and sagging of unconsolidated materials overlying gypsum karst through the cover/gypsum interphase (e.g. Cooper, 1998); catastrophic collapse of unconsolidated sediments into existing voids (Cooper, 1986, 1998; Yaoru and Cooper, 1997; Martinez and Boehner, 1997) or catastrophic collapse of competent strata into voids (breccia pipe propagation; Cooper, 1986; Ford, 1997; Martinez et al., 1998).

In this work a more simple classification attending to Bögli (1980) has been used. This classification points out to the surficial slope changes and separates the end-members of collapse and subsidence. This classification does not require the in-depth interpretation for the 3D karst structure. Following this description, the analyzed zone can be described in terms of two collapses surrounded by subsidence zones. The origin of the collapse geometries and

subsidence zones is related to the cohesion of cover materials. Subsidence zones can be interpreted as the vertical propagation of cavities located in a deep substratum (e.g., S0) but also as related to the lateral migration of granular deposits into underground collapses or deeper cavities (e.g., subsidence rings or envelopes, S1; e.g., Pueyo Anchuela, 2013).

The structural changes identified in the 3D geophysical model and their comparison with borehole data allow the interpretation of surficial slope changes in terms of a heterogeneous cover series sagging in response to an underground cavity. Progression of subsidence generates a dropout/suffusion sinkhole where granular materials can move laterally without vertical connection (e.g., subsidence ring surrounding a collapse) and depending on the cohesive carbonate crusts distribution. This interpretation depends upon the cohesion and internal friction angle of the cover, which configures the subsequently formed slopes and stabilization angles. In a high cohesive series, a collapse with subvertical walls is expected (similar to a collapse/caprock sinkhole or breccia pipe) contrasting with the opposite situation where the low cohesion should produce a wide sagging or dropout/suffusion sinkhole (Fig. 8). This two end-members and the studied case can be evaluated in terms of different stages of the same underground process with different surficial consequences depending upon the rheology of the cover series (Fig. 9a).

The rheology of the cover series strongly controls the affected volume. A vertical connection between a surficial collapse and the original cavity in the underground will present a general cylindrical geometry (cap-rock collapse sinkhole). At non cohesive materials a more stable gentle structure (drop-out/suffusion sinkhole; Fig. 9a) will progress with slope changes depending of the angle of internal friction. Any intermediate situation can be interpreted in terms of metastable situations due to the rheology of the cover rocks.

In the analyzed context, while a vertical caprock sinkhole can be geologically stable due to the strength of the affected materials, in cases where anisotropic behavior is found, they

can be considered as transient pictures until a more stable situation is reached (slope stability depending upon the internal friction angle of granular materials). The considered model has direct consequences in the evaluation of the affected volume varying from 2,000 to nearly 10,000 m^3 (Fig. 9a).

The interpretation of intermediate or metastable situations requires considering the potential surficial size increase and affected volume. This supports that any mitigation procedure needs to consider sectors wider than affected by the subsidence process at surface. In the studied case, the GPR 3D model of the volume of underground materials affected by karst processes shows a slightly more complex situation than the evaluated end-points. It is defined by collapse geometries surrounded by subsidence rings whose distribution is dependent on the irregular distribution of the carbonate crusts within the cover series (see. Fig. 9b).

The origin of the subsidence phenomena involves a time span longer than the analyzed range. The sudden beginning and the increase of activity during the last decades suggests an earlier origin. The irregular geometry of the water table, with sharp changes, even at directions normal to the general flow, suggests that water level deepens sharply in the southern collapse and disappears to the east of the studied area. A commonplace is that solution of evaporites is precluded by the presence of clay levels related to flood plain deposits and the weathered substratum, even when undersaturated meteoric waters (with high ability to dissolve underground materials) are present. Nevertheless, the collapse could connect both systems producing an increase of karst processes. The nearby position of an important irrigation channel that suffered subsidence could act as trigger for the first karst processes, while at this moment karst processes can be mainly associated with the natural water level. These data support that the evaluation of any geotechnical solution needs to consider the real and future

evolution of the subsidence phenomena with different scenarios regarding the water table and its connections.

6. 2 Evaluation of potential solutions

With the aim to propose a solution that guarantees the maintenance of the road in its current location avoiding the subsidence hazards, a revision of potential solutions considering the local geological characteristics has been done (Table 1). Mitigation treatments or construction styles have been applied to solve problems in karst areas. In general, all the applied approaches present positive and negative aspects and configure different hazard boundary conditions or surveillance works. While the different procedures are significantly site-dependent, some considerations can be obtained from carbonate and evaporite karst (Kannan; 1999; Waltham et al.,2005; Thomson et al., 1996; Paukštys et al., 1999; Cooper, 1995; Sorochan et al., 1985; Whaltam et al., 2005). The proposed solutions also need to prevent (or predict) the future development of new subsidente foci and the modification of the known ones (specifically changes related to the hydrogeological conditions, in the case of evaporite materials; De Bruyin and Bell, 2001; Waltham et al., 2005) and also to evaluate the social interest of the infrastructure and its cost-effective evaluation in the middle to long term scale.

The proposed solutions can be classified into two main groups depending upon the treated units. A first group attends to the evaluation of the karst problem in a static approach. In this case, solutions attempt to improve the mechanical properties of cover materials that have been affected by karst (through excavation and refill, compaction, grouting, reinforcement of the infrastructure, geogrids, claquage, compaction grouting, densification, etc.). These provisional solutions do not contribute to the stabilization of subsidence phenomena because they usually do not reach the causative depth (Bonaparte and Berg, 1987; Reuter and Tolmachehv, 1990; Sorochan et al., 1985: Whaltam et al., 2005). The case of

geogrids represents an invaluable procedure to avoid and prevent the appearance of catastrophic/sudden subsidence, and to control subsidence in continuous manner (Kempton et al., 1996; Cooper and Waltham, 1999; Paukštys et al., 1999; Cooper and Saunders, 2002; Jones and Cooper; 2005; Galve et al., 2012) but it does not represent a corrective measure. In some cases, these treatments can waterproof the studied area decreasing the solution in the substratum while in others, most notably grouting, changes in the hydrogeological behavior can lead to an increase of solution processes (e.g. Cooper, 1988; Waltham et al., 2005; Pueyo Anchuela, 2010a).

The second group attempts to individualize the construction from karst phenomena (foundations in non affected materials, distal footing; raft foundations, jackable foundations, reinforced strips or piling). This footing design is needed, as in the studied case, when the cover series does not offer a suitable medium for shallow foundations (due to lateral and vertical migration of cover series into underground cavities). In this situation, bulk grouts through boreholes or deep foundations are the most suitable (though expensive) solution when they do not change hydrogeological conditions (e.g. Johnson, 1989; 1998), they span over the whole problematic zone or can reach levels in the subsoil below the identified karstified zone (Waltham et al., 2005).

Traffic in the studied road was restricted since 2012 and solutions are being still analyzed. The main problems are related to subsidence and the vertical and horizontal extension of distress. Although traffic vibration can trigger collapses related to near surface cavities, in the analyzed case this subject is not considered significant when compared to the natural subsidence process. Borehole data reveal a general high strength that is compatible with required vertical loads between 3 and 5 MPa (Whaltam and Fookes, 2003) for the collapse of the carbonatic crust. However, the migration of unconsolidated materials, as identified in the studied zone, can be produced by vertical loads of only 0.2 MPa (Pando et al.,

2013), with independence of their static geotechnical evaluation that, in general, shows medium to high strength values.

From the previously described solutions, of usual application worldwide, two of them have been evaluated in the studied case: the integration of reinforced structures over grouted or compacted soils and geogrids or the use of rigid structures supported on deep foundations (Siegel et al., 2001). In the side of safety the most efficient solutions should be related to drilled shafts/piles supporting a reinforced structure (raft or mattresses; Fig. 10). This solution should benefit from the correct footing in the non karstified materials in the subsoil and deeper than the lower contact of the cover rocks (taking special attention at the related hydrogeological changes and testing below the piles). The associated raft should span respect the identified karst problems to avoid subsidence problems surrounding it. The independent behavior of the structure with respect to the subsidence processes recorded by both cover and substratum materials requires surveillance for the identification of cavities below the rafts and the appearing of subsidence phenomena at marginal areas (lateral migration of the subsidence cones out of the known subsidence zones). This solution that potentially represents low-cost in the surveillance and reparations requires an important investment in the first steps of construction. This proposal was assessed consisting of a rigid structure with an armored concrete slab plate supported on piles 35-40 meters long, with consequent transition slabs in both longitudinal and transverse joint sections. This deep foundation would directly transmit the load to the unaltered Cenozoic substratum. The estimated budget for the implementation of this structural solution in the affected area is 500,000 €. This solution will stabilize the central and most affected area, although the outermost affected areas could still suffer subsidence due to the centrifuge evolution.

The second evaluated proposal considers the improvement of surface materials, surficial grouting or geotextiles/geomembranes. However, they only represent temporary

solutions that must be subjected to surveillance and continuous reparations. However, at roadways of low importance and with low traffic density, they can be used as temporary procedures to avoid catastrophic subsidence processes. Geogrids permit this kind of solution, although the sinkhole size and depth should require the construction of a 2 m high reinforced embankment (due to planning restrictions) with a basal excavation of 2 m. The excavation and retirement of the carbonate crusts from the underground to avoid cover cap-rocks, in the studied case, cannot be performed if the security of the buildings neighboring the road must be maintained. A preliminary calculation shows that geogrid requires, for the studied case and considering the local geological and construction characteristics, a tensile load greater than 2000 kN/m, for the expected road traffic. This value is out of the usual geogrid products. Furthermore, although it could prevent sudden collapses, this would not be a final solution because the source of the subsidence process would continue causing vertical ground movements whose lateral progression could exceed the limits of the geogrid and lowering the reinforced embankment. In this situation, to avoid strengthening of the geogrid during continuous reparations the excavation of the road at each operation is crucial. This aspect will increase in middle to long term the needed investment.

Any solution should consider three main aspects: i) the stabilization of the infrastructure, ii) precluding future development of subsidence phenomena and a surveillance routine and iii) to perform an economic evaluation in terms of infrastructure and social relevance (Fig. 11). The available budget for the reparation of a first order infrastructure is not the same than a local road with limited traffic or where the adopted solution must take into account surveillance and future reparations. Beyond these aspects, the type of hazards must also be considered, because continuous subsidence can be mitigated through continuous reparations, whereas a sudden, catastrophic collapse can represent a non-admissible hazard.

At the beginning of this work, and making reference to the usual approaches in infrastructure planning, the most efficient solution presented was to avoid the construction over known hazardous areas. This scenario was not *a priori* considered because karst problems appeared after construction. However, the integrated evaluation of the related costs and the potential solutions, surveillance and mitigation procedures, can orient about the possibility of road relocation. In fact, the economic evaluation with middle to long-term perspective led the town hall of Gallur to exclude the studied zone and its surrounding areas from the new urban planning regulations. The relocation of the road is not as easy at this moment as it could be during former stages of urban planning because the network of infrastructures associated to the road should also be modified. In the scenario of re-locating the road to avoid hazardous areas, a continuous surveillance of the old road, even without traffic, is necessary to avoid or predict subsidence processes or collapses.

6. Conclusions

Construction or mitigation solutions in sectors affected by evaporite karst processes represent a difficult task in geotechnical practice. In the analyzed case, the generation of cavities in the soluble substratum and their propagation to the surface through a cover series with contrasting geomechanical properties, makes difficult its 3D evaluation. Subsidence and collapse geometries at surface are succeeded, in the underground, by a complex 3D structure with tens of thousands cubic meters affected by the karst process and metastable situations due to the cohesive caprocks within the cover. Data integration has permitted to evaluate the applicability of GPR in order to draw the structure of the cover rocks affected by karst processes and to describe metastable trends between isolated vertical collapses (breccia pipes) and inverse Gaussian structures typical of suffusion sinkholes. These trends can be used to predict subsequent size increase and to define sectors to be included in the engineering solutions with independence of the surficial indicators at present conditions.

The revision of mitigation measurements for this kind of problems reveals the high complexity for determining the most efficient, economic, socially acceptable and safe solution to be applied. A sketch of the potential elements to be analyzed, a review of potential solutions to be applied and their expected success and limitations have been analyzed. For the studied case, the local characteristics of the studied zone permitted to recommend a relocation of the infrastructure as the most economic and safe alternative. The walkthrough analysis developed in this study can be used as a guide adaptable to other settings where the optimum solution can be different. On the other hand, this kind of analysis, where population is included in the decision making, can permit the increase of public participation and the comprehension of the adopted solutions with short to long term perspective.

Acknowledgements

Geotransfer research group founded by the Aragon Government and European Social Founding (E27) and project CGL2011-23717 of the Ministry of Economy and Competitiveness of Spain supported this research. Authors want to thank the support from town hall and local authorities from Gallur (Zaragoza), their interest in sharing and public participation of inhabitants in this analyzed subject and to Diputación Provincial de Zaragoza. Authors want to thank editor and two anonymous reviewers by their constructive revision of the first manuscript version.

References

Beck, B.F., 2004. Soil piping and sinkhole failures. In: White WB (eds) Encyclopedia of caves. Elsevier, Nueva York, p 523–528.

Benito, G., Pérez-González, A., Gutiérrez, F., Machado, M.J., 1998. River response to Quaternary subsidence due to evaporite solution (Gállego River, Ebro Basin, Spain). Geomorphology. 22, 243–263.

Bögli, A., 1980. Karst hydrology and physical speleology. 284. Springer-Verlag. Berlin.

Bonaparte, R., Berg, R.R., 1987. The use of geosynthetics to support roadways over sinkhole prone areas. In: Beck, B.F., Wilson, W.L., (eds) Karst hydrogeology: engineering and environmental applications, 437-445. Balkema, Rotterdam.

Castiella, J., del Valle, J., Ramírez del Pozo, D., 1977. Hoja y memoria del mapa geológico de España, 1:50.000. Hoja 321 (Tauste). Instituto Geológico y Minero de España. Madrid. 18 p.

Cooper, A.H., Saunders, J.M., 2002. Road and bridge construction across gypsum karst in England. Engineering Geology. 65, 217-223.

Cooper, A.H., Waltham, A.C., 1999. Subsidence caused by gypsum dissolution at Ripon, North Yorkshire. Quarterly Journal of Engineering Geology. 32, 305–310.

Cooper, A.H., 1986. Subsidence and foundering of strata caused by the dissolution of Permian Gypsum in the Ripon and Bedale areas, North Yorkshire. In: Harwood, G.M., Smith, D.B. (Eds.), The English Zechstein and Related Topics. Geological Society, London, Special Publication, vol. 22, 127– 138.

Cooper, A.H., 1998. Subsidence hazards caused by the dissolution of Permian gypsum in England: geology, investigations and remediation. Geological Society Engineering Group Special Publication. 15, 265-275.

Cooper, A.H., 1995. Subsidence hazards due to the dissolution of Permian gypsum in England: investigation and remediation. In: Beck, F.B. (Ed.), Karst Geohazards: Engineering and Environmental Problems in Karst Terrane. Proceedings of the Fifth Multidisciplinary Conference on Sinkholes and the Engineering and Environmental Impacts of Karst, Gatlinburg, TN, 2–5 April 1995, A.A. Balkema, Rotterdam. 23–29.

De Bruynm I.A., Bell, F. G., 2001. The occurrence of sinkholes and subsidence depressions in the Far West Rand and Gauteng Province, South Africa, and their engineering implications. Environmental Engineering Geoscience. 7, 281-295.

Ferrero, A.M., Segalini, A., Giani, G.P., 2010. Stability analysis of historic underground quarries. Comput. Geotech. 37, 476–486.

Ford, D.C., 1997. Principal features of evaporite karst in Canada. Carbonates and Evaporites. 12, 15– 23.

Galve, J.P., Gutiérrez, F., Guerrero, J., Alonso, J., Diego, I., 2012. Application of risk, cost-benefit and acceptability analysis to identify the most appropiate geosyntethic solution to mitígate sinkhole damage on roads. Engineering Geology. 145-146, 65-77.

Galve, J.P., Gutiérrez, F., Lucha, P., Bonachea, J., Remondo, J., Cendrero, J., Gutiérrez, M., Gimeno, M.J., Pardo, G., Sánchez, J.A., 2009. Sinkholes in the salt-bearing evaporitic karst of the Ebro river valley upstream of Zaragoza city (NE Spain). Geomorphological mapping and analysis as a basis for risk management. Geomorphology. 108, 145–158.

Gao, Y., Alexander, E.C., Barnes, R.J., 2005. Karst database implementation in Minnesota: analysis of sinkhole distribution. Environmental Geology. 47, 1083-1098.

García Castellanos, D., Vergés, J., Gaspar-Escribano, J.M., Clething, S., 2003. Interplay between tectonics, climate and fluvial transport during the Cenozoic evolution of the Ebro Basin (NE Iberia). J. Geophys. Res. 108 (B7): 2347.

Gil, H., Luzón, A., Soriano, M.A., Casado, I., Pérez, A., Yuste, A., Pueyo, E.L., Pocoví, A., 2013. Stratigraphic architecture of alluvial–aeolian systems developed on active karst terrains: An Early Pleistocene example from the Ebro Basin (NE Spain). Sedimentary Geology. 296, 122-141

Greenfield, S.J., Shen, C.K., 1992. Foundation Problems in Soils. Prentice Hall, Englewood Cliffs, NF, 149–163.

Gutiérrez, F., Guerrero, J., Lucha, P., 2008. Quantitative sinkhole hazard assessment. A case study from the Ebro Valley evaporite alluvial karst (NE Spain). Nat. Hazards. 45, 211–233.

Gutiérrez, F., Galve, J.P., Lucha, P., Castañeda, C., Bonachea, J., Guerrero, J., 2011. Integrating geomorphological mapping, trenching, InSAR and GPR for the identification and characterization of sinkholes: A review and application in the mantled evaporite karst of the Ebro Valley. Geomorphology. 134, 144-156

Johnson, K.S., Neal, J.T., 2003. Evaporite karst and engineering/environmental problems in the United States. Oklahoma Geological Survey Circular, 109. 353 pp.

Johnson, K. S., 1989. Salt dissolution, interstratal karst and ground subsidence in the northern part of the Texas Panhandle. In: Beck, B.F., (ed). Engineering and Environmental Impacts of Sinkholes and Karst, pp. 115-121. Balkema, Rotterdam.

Jones, C. J. F. P., Cooper, A.H., 2005. Road construction over voids caused by active gypsum dissolution with an example from Ripon, North Yorkshire, England. Environmental Geology. 48 (3), 384-394.

Kannan, R.C., 1999. Designing foundations around sinkholes. Engineering Geology. 52, 75-82.

Kempton, G.T., Lawson, C.R., Jones, C.J.F.P., Demerdash, M., 1996. The use of geosynthetics to prevent the structural collapse of fills over areas prone to subsidence. In: De Groot, M.B., Den Hoedt, G., Termaat, R.J. (Eds.), Geosynthetics: Applications, Design and Construction. A.A. Balkema, Rotterdam, 1086.

Kozary, M.T., Dunlap, J.C., Humphrey, W.E., 1968. Incidence of saline deposits in geologic time. Geological Socierty America Special Paper. 88, 43-57.

Lamelas, M.T., Marinoni, O., Hopper, A., de la Riva, J., 2008. Doline probability map using logistic regression and GIS technology in the central Ebro Basin (Spain). Environ. Geol. 54, 963–977.

Lamont-Black, J., Younger, P.L., Forth, R.A., Cooper, A.H., Bonniface, J.P., 2002. A decision logic framework for investigating subsidence problems potentially attributable to gypsum karstification. Engineering Geology. 65 (2–3), 205–215.

Luzón, A., 2005. Oligocene–Miocene alluvial sedimentation in the northern Ebro Basin, NE Spain: Tectonic control and palaeogeographical evolution. Sedimentary Geology. 177, 19-39

Luzón, A., Pérez, A., Soriano, M.A., Pocoví, A., 2008. Sedimentary record of Pleistocene paleodoline evolution in the Ebro basin (NE Spain). Sedimentary Geology. 205, 1-13

Macau, F., Riba, O., 1962. Situación, características y extensión de los terrenos yesíferos en España. I Col. Intern. Obras Públ. en terrenos yesíferos. Serv. Geol. O. Públ. Madrid, 28 pp.

Marker, B.R., 2010. Review of approaches to mapping of hazards arising from subsidence into cavities. Bull. Eng. Geol. Environ. 69, 15-183.

Martinez, J.D., Boehner, R., 1997. Sinkholes in glacial drift underlain by gypsum in Nova Scotia, Canada. Carbonates and Evaporites. 12 (1), 84–90.

Martinez, J.D., Johnson, K.S., Neal, J.T., 1998. Sinkholes in evaporite rocks. American Scientist. 86, 39– 52.

Mochales, T., Casas, A.M., Pueyo, E.L., Pueyo, Ó., Román, M.T., Pocoví, A., Soriano, M.A., Ansón, D., 2008. Detection of underground cavities by combining gravity, magnetic and ground penetrating radar surveys: a case study from the Zaragoza area, NE Spain. Environmental Geology. 53 (5), 1067-1077.

Moreno Merino, L., Garrido Schneider, E.A., González, Azcón de Aguilar, A., Durán Valsero, J.J., 2008. Hidrogeología urbana de Zaragoza. Instituto Geológico y Minero de España, Madrid. 200 pp

Neal, A., 2004. Ground penetrating radar and its use in Sedimentology: principles, problems and progress. Earth-Science Reviews. 66, 261-330

Pando, L., Pulgar, J.A., Gutiérrez-Claverol, M., 2013. A case of man-induced ground subsidence and building settlement related to karstified gypsum (Oviedo, NW Spain). Environmental Geology. 68, 507-519.

Pardo, G., Arenas, C., González, A., Luzón, A., Muñoz, A., Pérez, A., Pérez-Rivarés, F.J., Vázquez-Úrbez, M., Villena, J., 2004. La Cuenca del Ebro. Geología de España, IGME 533–543.

Parise, M., Lollino, P., 2011. A preliminary analysis of failure mechanism and man-made underground caves in southern Italy. Geomorphology. 134, 132-143.

Paukštys, B., Cooper, A.H., Arustiene, J., 1999. Planning for gypsum geohazards in Lithuania and England. Engineering Geology. 52, 93– 103.

Paukštys, B., Cooper, A.H., Arustienne, J., 1997. Planning for gypsum geohazards in Lithuania and England. In: Beck, B.F., Stephenson, J.B. (Eds.), The Engineering Geology and Hydrogeology of Karst Terranes. Proceedings of the 6th Multidisciplinary Conference on Sinkholes and the

Engineering and Environmental Impacts of Karst, Springfield, MO, 6 – 9 April, 1997. Balkema, Rotterdam. 127– 135.

Peck, R.B., 1969. Deep Excavations and Tunneling in Soft Ground. En Proceedings of the 7th International Conference in Soil Mechanics Foundation. Engineering, State of the Art. 225-250.

Pérez Rivarés, F.J., Garcés, M., Arenas, C., Pardo, G., 2002. Magnetocronología de la sucesión miocena de la Sierra de Alcubierre (sector central de la Cuenca del Ebro). Rev. Soc. Geol. Esp. 15 (3–4), 217–231.

Pueyo Anchuela, Ó., Pocoví Juan, A., Soriano, M.A., Casas-Sainz, A.M., 2009. Characterization of karst hazards from the perspective of the doline triangle using GPR- Examples from Central Ebro Basin (Spain). Engineering Geology. 108, 225-236.

Pueyo Anchuela, Ó., Pocoví Juan, A., Casas-Sainz, A.M., Ansón-López, D., Gil-Garbí, H., 2013. Actual extension of sinkholes: considerations about geophysical, geomorphological and field inspection techniques in urban planning projects in the Ebro basin (NE Spain). Geomorphology. 189, 135-149.

Pueyo Anchuela, Ó., Casas Sainz, A.M., Pocoví Juan, A., Gil, H., Calvín, P., 2014a. Characterization of the karstic process in an urban environment using GPR surveys. Journal of Materials in Civil Engineering. 26 (8) 05014004.

Pueyo Anchuela, Ó., Luzón, A., Gil Garbi, H., Pérez, A., Pocoví, A., Soriano, M.A., 2004b. Combination of electromagnetic, geophysical methods and sedimentological studies for the development of 3D models in alluvial sediments affected by karst (Ebro Basin, NE Spain). Journal of Applied Geophsics. 102: 81-95

Quirantes, J., 1978. Estudio sedimentológico y estratigráfico del Terciario continental de los Monegros. Ph D Thesis Publication 681, Institución Fernando el Católico (CSIC), Zaragoza.

Reuter, F., Tolmachev, V.V., 1990. Bauen und Bergbau in Senkungs und Erdfallgebieten, Eine Ingenieur geologie des Karstes. Schriftenr. Geol. Wiss., vol. 28, Academie-Verlag, Berlin.

Salvany, J.M., 2009. Geología del yacimiento glauberítico de Montes de Torrero (Zaragoza). Prensas Universitarias de Zaragoza (80 pp).

Salvany, J.M., García–Veigas, J., Ortí, F., 2007. Glauberite–halite association of the Zaragoza Gypsum Formation (Lower Miocene, Ebro Basin, NE Spain). Sedimentology. 54, 443–467.

Shalev, E., Lyakhovsky, V., 2012. Viscoelastic damage modeling of sinkhole formation. Journal of Structural Geology. 42, 163-170.

Siegel, T.C., McCracken, D.W., 2001. Geotechnical characterization and modeling of a shallow karst bedrock site. In: Beck, B.F., Herring, J.G., (eds) Geotechnical and Environmental Applications of Karst Geology and Hidrology. Pp. 169-172. Balkema: Lisse.

Simón J.L., Soriano M.A., 2002. Actual and potential doline subsidence hazard mapping: case study in the Ebro Basin, Spain In: Bobrowsky PT (ed) Geoenvironmental mapping: methods, theory and practice AA Balkema (Lisse), pp 649–666

Simón, J.L., Soriano, M.A., Arlegui, L.E., Gracia, J., Liesa, C.L., Pocoví, A., 2008. Space-time distribution of ancient and active alluvial karst subsidence: examples from the central Ebro Basin, Spain. Environmental Geology. 53, 1057-1065.

Soriano, M.A., 1990. Geomorfología del sector centro-meridional de la Depresión del Ebro. Diputación Provincial de Zaragoza.

Soriano, M.A., Simón, J.L., 2002. Subsidence rates and urban damages in alluvial dolines of the central Ebro Basin (NE Spain). Environ. Geol. 42, 476–484.

Sorochan, E.A., Troitzky, G.M., Tolmachov, V.V., Khomenko, V.P., Kkepokov, S.N., Metelyuk, N.S., Grigoruk, P.D., 1985. Antikarst protection for buildings and structures. In: Proceedings of

the Eleventh International Conferenceon Soil Mechanics and Foundation Engineering, San Francisco, 12–16 August 1985, Balkema, Rotterdam, 2457–2460.

Sowers, G.F., 1986. Correction and protection in limestone terrane. In: Proc. First Multidisciplinary Conference on Sinkholes, Orlando, FL, A.A. Balkema, Rotterdam, pp. 373–378.

Sowers, G.F., 1996. Building on Sinkholes. ASCE Press, New York. 202 pp.

Thierry, P., Prunier-Leparmentier, A.M., Lembezat, C., Vanoudheusden, E., Vernux, J.F., 2009. 3D geological modeling at urban scale and mapping of ground movement susceptibility from gypsum dissolution: The Paris example (France). Engineering Geology. 105, 51-64.

Thomson, A., Hine, P.D., Greig, J.R., Peach, D.W., 1996. Assessment of subsidence arising from gypsum dissolution. Technical Report for the Department of the Environment. Sumonds Group Ltd. Eas Gristead.

Van Zuidam, R.A., 1976. Geomorphological development of the Zaragoza region, Spain. Processes and landforms related to climatic changes in a large Mediterranean river basin. International Institute for Aerial Survey and Earth Sciences (ITC), Enschede.

Waltham, T., Bell, F., Culshaw, M., 2005. Sinkholes and subsidence. Karst and cavernous rocks in engineering and construction. Praxis Publishing Ltd. Chichester, UK. 382 p.

Whaltam, A.C., Fookes, P.G., 2003. Engineering classification of karst ground conditions. Quaterly Journal Engineering Geology Hydrogeology. 36, 101-118

Yaoru, L., Cooper, A.H., 1997. Gypsum karst geohazards in China. In: Beck, B.F., Stephenson, J.B. (Eds.). The Engineering Geology and Hydrogeology of Karst Terranes. Proceedings of the 6th Multidisciplinary Conference on Sinkholes and the Engineering and Environmental Impacts of Karst, Springfield, MO, 6 – 9 April, 1997, pp. 117– 126.

Zhou, W., Beck, B.F., Adams, A.L., 2003. Application of matrix analysis in delineating sinkhole risk areas along highway I-70 near Frederick, Maryland. Environmental Geology. 44, 834-842.

Zhou, W., Beck., B.F., 2008. Management and mitigation of sinkholes on karst lands: an overview of practical applications. Environmental Geology. 55, 837-851.

Figure Captions

Figure 1.- Geological map with the location of the studied zone (modified and updated from Castiella et al., 1977). Units are grouped either into cover (Quaternary) or consolidated (substratum) rocks.

Figure 2.- (a,b,c) Aerial photographs from 1984,1998 and 2012. Note the appearing of subsidence depressions at the flight from 1998. At (c) the studied zone and the traffic restricted area are marked.

Figure 3.- Field photographs from the studied zone. (a) Oblique view from the analyzed road with the main cracks and subsidence areas. (b) Detail from surficial cracks, (c) Photographs of the buildings located at the SE corner of the studied zone where the main wall cracks are highlighted. (d) Photograph taken from drone flight in 2014 in which the most evident cracks and slope changes are marked. (e) and (f) details of the two observed main subsidence zones

Figure 4.- (a) Location of the studied GPR profiles that were carried out with the 100 and 250 MHz (profiles marked at the figure are done with the 100 MHz antennae). (b) Comparison of the same transects for 100 and 250 MHz in the analyzed road (profile 3 done over the road). (**c**) Examples of longitudinal profiles done over the road. Reference lines, net interruptions (dashed lines) and hyperbolic anomalies (discontinuous lines) are included. Besides these lines, a reflector usually not identified at the whole profile is also marked (lower

northern part of the profiles). (d) GPR profiles (100 MHz) done out perpendicular to profiles from (c) ;profiles 21 and 24; see location in fig. 4a).

Figure5.- Borehole logs and dynamic resistance of the different units (SPT: standard penetration test, for the sum for both intermediate analyzed intervals are included). Inset photographs from the obtained cores. Note the powder aspect of carbonate crusts and the identification of cemented structures at some of the logs (see, S2 photograph at 3.6 meters).

Figure 6.- (a) Superposition of borehole logs over the GPR-profiles and their proposed depth (propagation velocity has been calculated from the fitting of hyperbolic anomalies with a mean value of 110 m/μs; depth has been contrasted with boreholes identifying the correlation between water level with the position of the identified deep reflector. (b) Obtained model from defined domains at GPR profiles of reflector tilting, interruption and level accommodation (subsidence affecting to the cover materials in a non cohesive manner) against the deeper levels where, even with net lateral contacts, there is not a change of the underground structure (dip change of reflectors or accommodation).

Figure 7.- (a) False relief model obtained from the analysis of GPR profiles between affected and non-affected cover materials by sagging processes. In the illustration both subsidence rings and collapses are marked. This model represents a pseudo 3D integration of 2D GPR features where the interpolation reference pixel has been established in the range of profile separation. (b) Same model than (a) with isopachs of the affected materials (the correlation of TWT intervals and depths are included). References are included to collapses and subsidence –inner or external- rings. (c) Comparison of the 3D GPR model over the aerial photograph and the mapped cracks and slope changes from fig. 3d.

Figure 8.- Simplified conceptual model relating the sinkhole development to the appearing of cavities in the consolidated substratum (the hypothesis of an ellipsoidal cavity has been chosen for simplicity in the sketch, while interconnection of different cavities,

solution through the contact between the soluble and the insoluble units can be the origin of an underground cavity). From this general model, depending upon the rheology of the cover rocks, different surficial and structural changes can be expected from a direct connection of a vertical collapse through a cohesive level (e.g. breccia pipe, collapse or caprock sinkhole) to a non cohesive behavior (suffusion, dropout or subsidence sinkhole). Intermediate cases with cemented levels within the cover rocks are also considered. Note that the surficial extension, involved cover series and surficial rate of subsidence phenomena due to the same underground cavity can drastically change depending upon the cover rheology.

Figure 9.- (a) Plot that includes the evaluation of affected areas and volumes for different types of sinkholes including caprock/collapse sinkholes (cohesive) to dropout/suffusion (non cohesive materials). The calculation has been established for the data analyzed in the studied case, considering the identified radius and depth to the consolidated substratum. The profiles for the studied case represent the characteristics for the granular characteristics in the studied case and where lower resistance can be expected for materials with lower internal angle of friction. This evaluation needs to be constrained with data from the analyzed cases, but considering the local characteristics can be used as an approach to identify the metastable situation represented at cases where caprocks within the cover series has not permitted the complete cover migration (unstable or intermediate cases). (b) At the studied case, the evaluation can be seen as more complex having collapses within subsidence zones and more than one collapse structure, due to the presence of geomechanical anisotropies within the cover series.

Figure 10.- Sketch following the conceptual models included at fig. 8 with the potential evaluation of mitigation measurements. Different solutions including geotextiles, grouting and piles are considered. The evaluation of the different solutions includes both the temporal and definitive solution and the model constrained for only surficial evidences and potential

affected volumes in the underground. In the intermediate case, the plots from grouting through boreholes are included just to evaluate the injection required; the weight increase and hydrogeological changes must also be considered in the evaluation of this kind of solutions.

Figure 11.- Factors needed to be evaluated in the consideration of procedures and mitigation tasks along roads. Budget is constrained by the infrastructure relevance and by its social interest. In this case, the temporary solution (static evaluation) requires a lower budget, but each time of reparation represents the same budget inversion to avoid strength increase. Dynamic approaches require a higher budget inversion at the beginning, while mitigation and surveillance procedures are, in general, lower than for temporal solutions. In the plot the evaluation of the potential infrastructure relocation that present a shared field of inversion between temporal and long-term solutions is included.

Table 1.- Summary of evaluation of pros and cons for the different potential solutions that can be applied at roads over evaporite karstified environments.

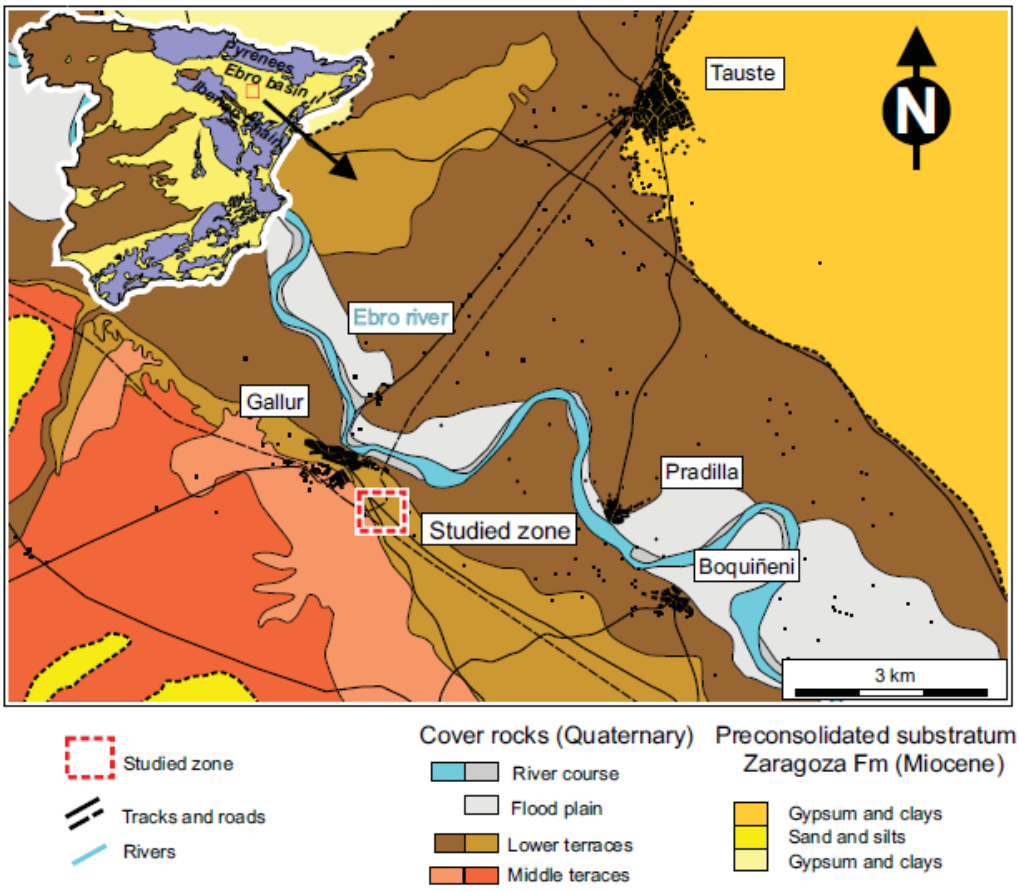

Figure 01.-

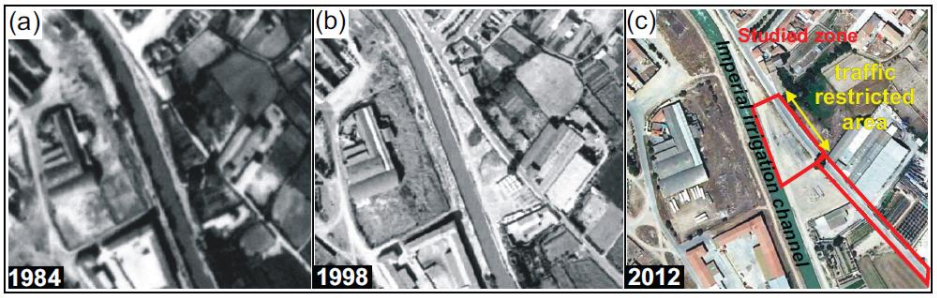

Figure 2.-

Figure 3.-

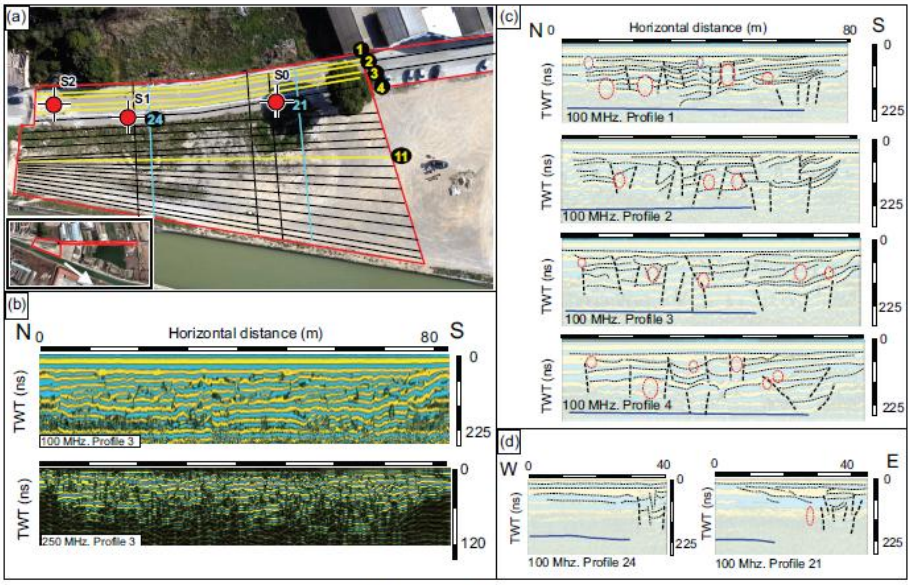

Figure 04.-

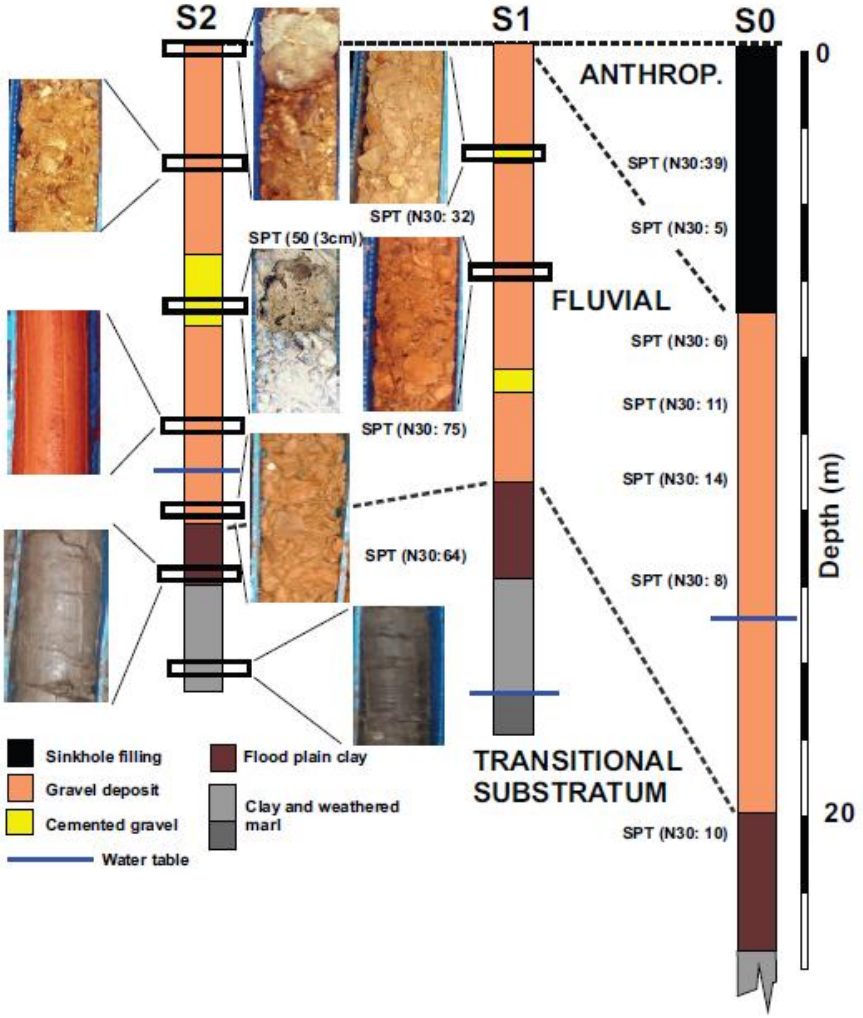

Figure 5.-

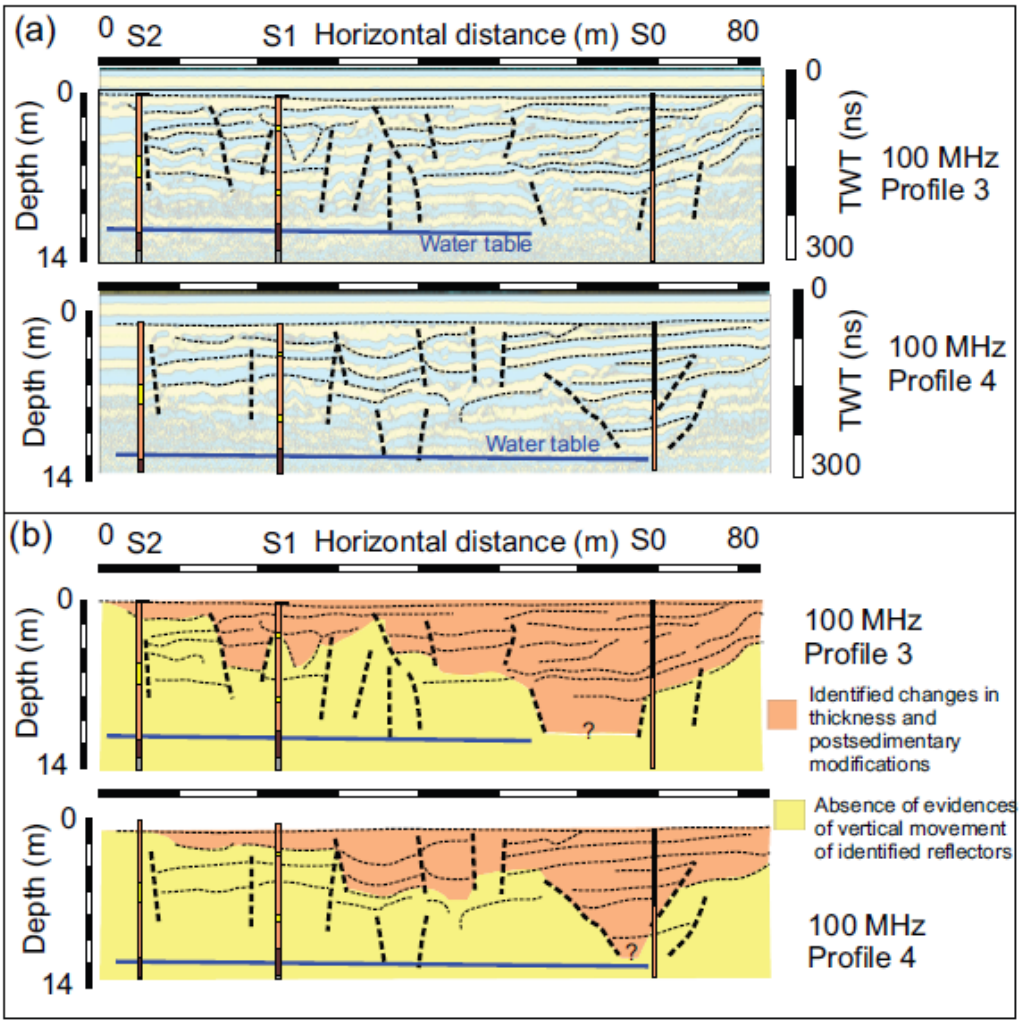

Figure 06.-

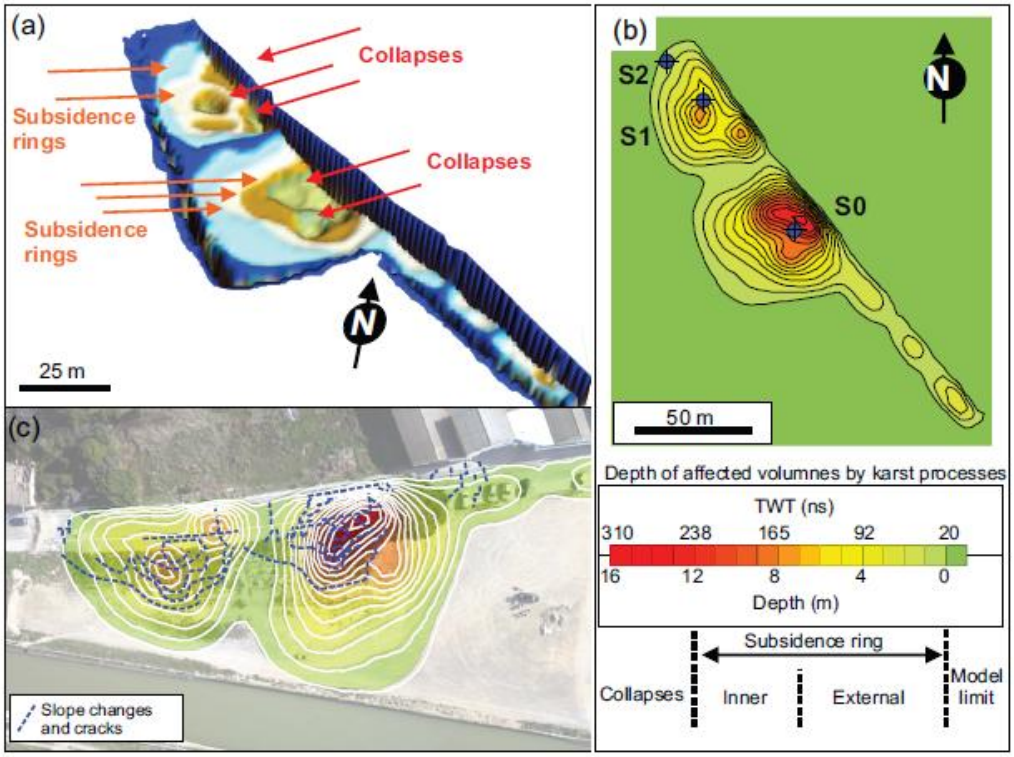

Figure 7.-

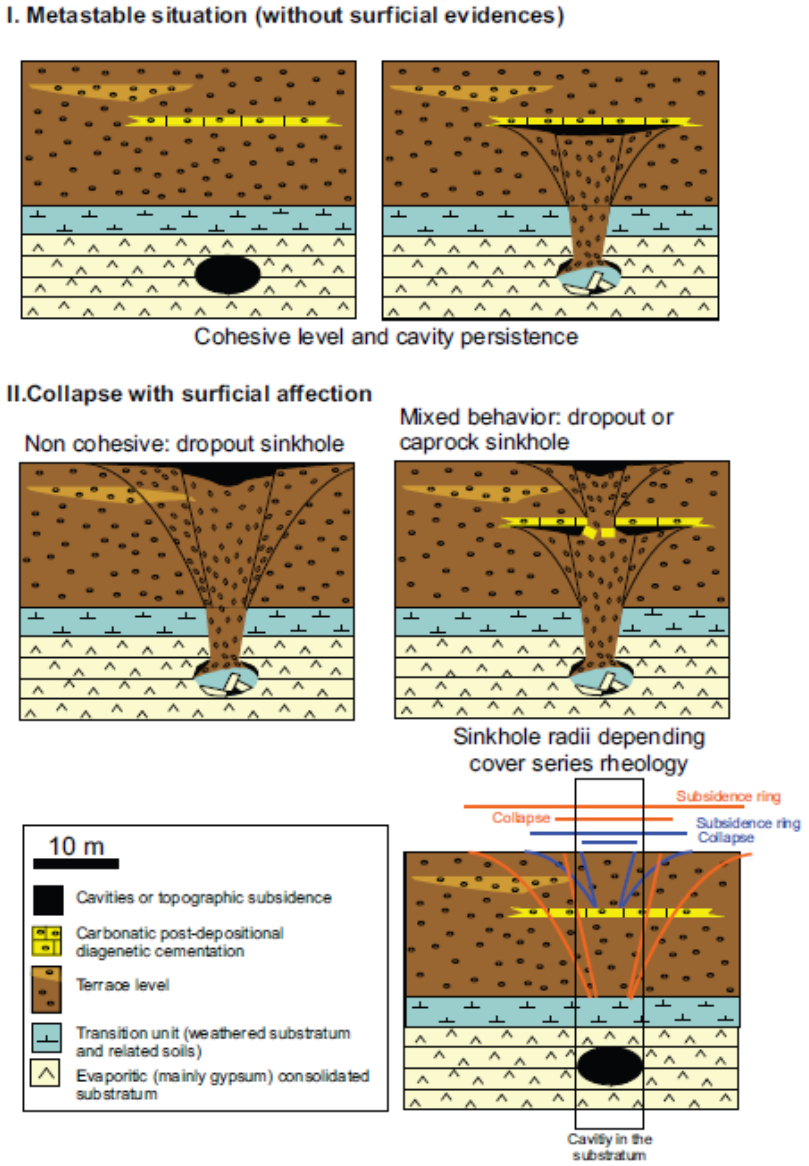

Figure 8

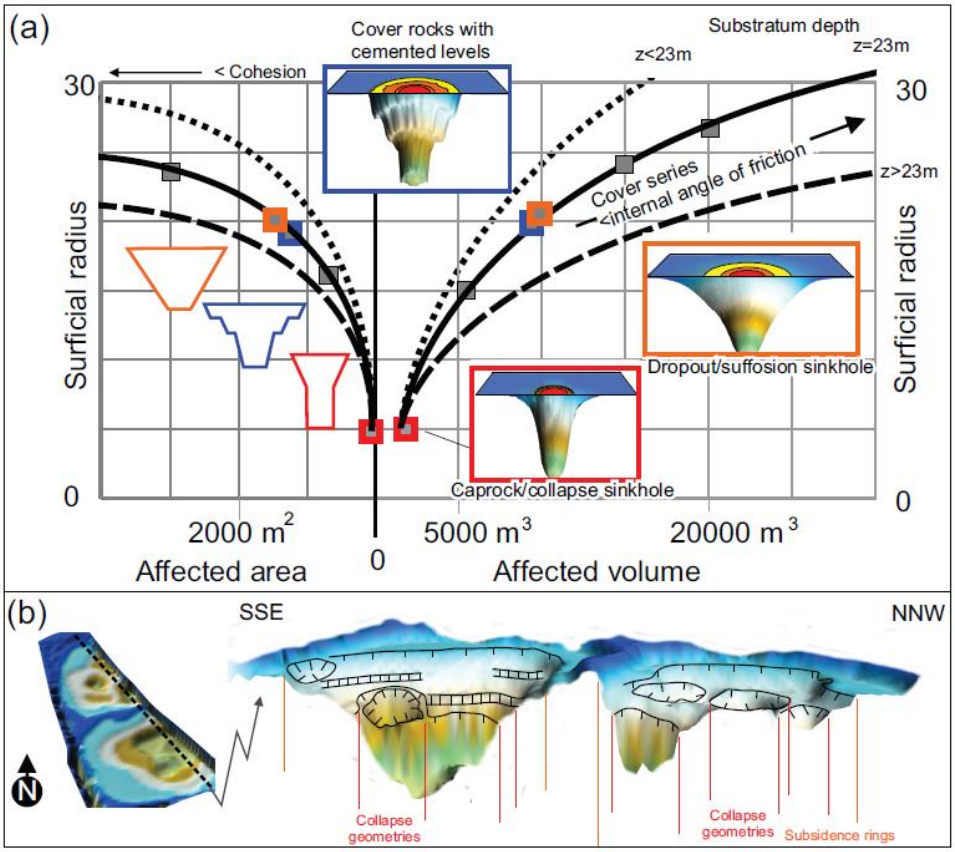

Figure 9

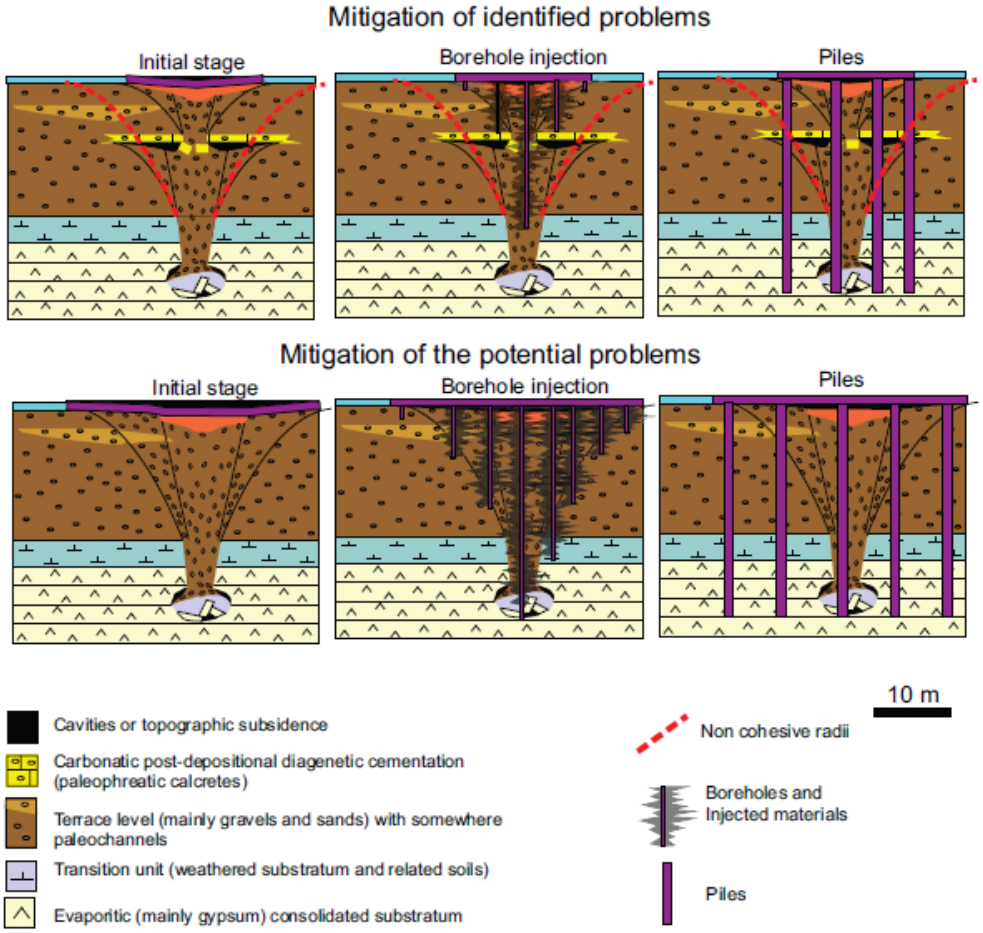

Figure 10.-

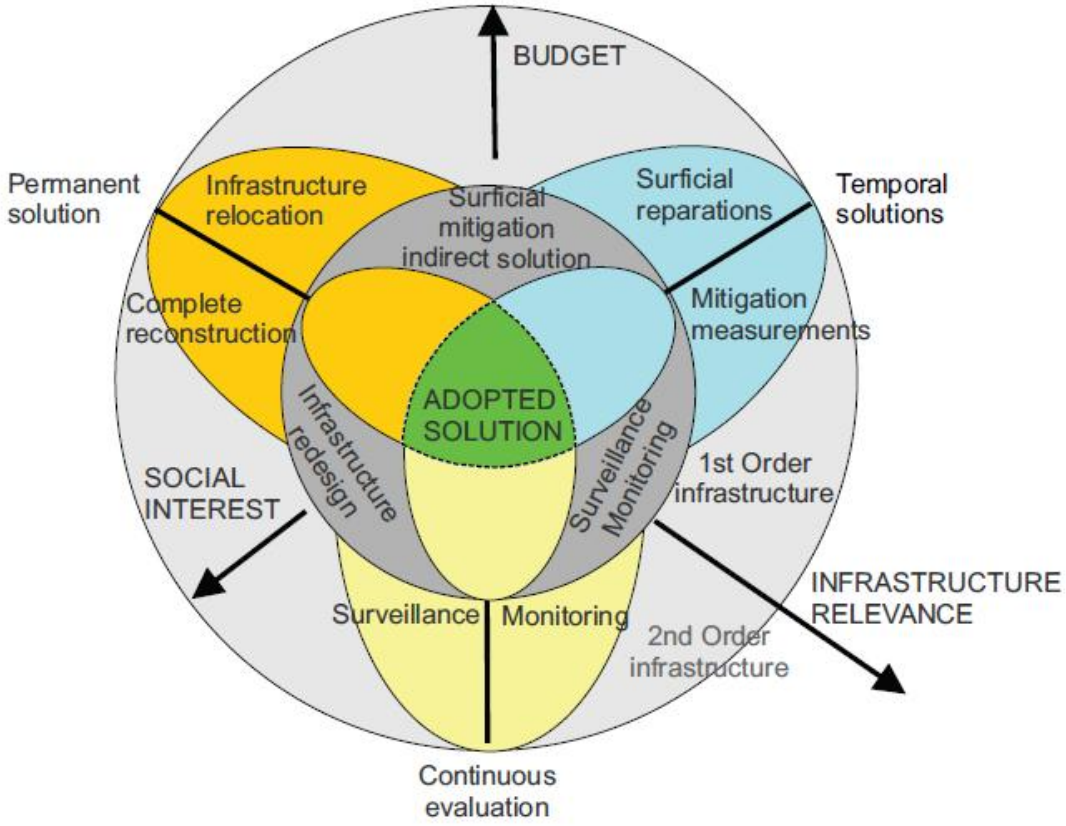

figure 11

Proposed solution		Pro-aspects	Against-aspects	Integrated measurements Surveillance tasks	Static/ Dynamic	Hazard changes	Mitigation cost	Future costs
Surficial reparation and filling		Fast and economic Detention of lateral migration	Temporal	Mitigation measurements Traffic bypass mandatory	S	–		
Soil compaction		Strength increase	Temporal	Success only at collapses	S	Potential change of rheology subsidence vs. collapses		
Soil remove and reconstruction		Strength increase	Temporal hydrogeological changes focusing infiltration	Success only at collapses	S	Potential change of rheology subsidence vs. collapses		
Soil Grouting		Strength increase	Increase of rigid behavior Hydrogeological changes	Difficult surveillance No mitigation of treated materials		Potential change of rheology subsidence vs. collapses		
	floats	Non significant weight increase			S	Increase of hazards at marginal areas from grouting		
	high density (concrete)	Increase of rigid behavior Weight increase Hydrogeological changs Permanent change (density)		Surveillance surrounding treated zones	S	Appearing of sudden collapses from underlying grouted materials		
	deep grouts			Surveillance surrounding treated zones Hydrogeological changes surveillance (infiltration,erosion or solution increase)	S	Weight increase can produce collapses of cavities in the substratum Focus of water table and its flowpath generating increase of karst activity (radius increase and activity)		
Infrastructure reinforcement	rigid	Indivualization of subsidence affecting the infrastructure	Surficial absence of activity record	Surveillance below rigid structures	S	Potential change of rheology subsidence vs. collapses		
	ductile/geogrids	Avoid sudden collapes or subsidence surficial evidences	Complete reconstruction Apparent hazard decrease	Surveillance from the surface to identify precursory karstic evidences	S			
Foundations	Shallow isolated	Surficial temporal stabilization	Footing at potential unstable materials Local failure of structure	Surveillance below footings	S	Potential change of rheology subsidence vs. collapses		
	Shallow: mattresses;rafts	Surficial temporal stabilization	Footing at potential unstable materials	Surveillance below matresses	S			
	Deep isolated (piles)	Real etabilization Complete independence respect cover	Hydrogeological changes Focusing of infiltration Cavities below piles Erosion at high hydraulic conditions surrounding piles.	Surveillance of piles and between them after construction Surveillance of hydrogeological conditions changes related to piles	D	Increasing of karst activity (hydrogeological) Failure of piles due to cavities		
	Integrated deep and shallow	Real stabilization Complete independence respect cover	Hydrogeological changes Focusing of infiltration Cavities below piles Erosion at high hydraulic conditions surrounding piles.	Surveillance of piles and between them after construction Surveillance of hydrogeological conditions changes related to piles	D	Collapses or subsidence surrounding treated sectors		

Table 01

Highlights

· Volume calculation of affected cover series at mantled karst.

· Evaluation of engineering solutions over gypsum karst

· Integrated analysis including geomorphological, geological, surficial, geophysical and geotechnical data.

· Decision making and temporal, economic and integrated evaluation.